

## **THERMAL DEFORMATION ANALYSIS OF ABB IRB 140 INDUSTRIAL ROBOT**

Cozmin CRISTOIU<sup>1</sup>, Miron ZAPCIU<sup>2</sup>, Adrian Florin NICOLESCU<sup>3</sup>, Cristina PUPAZA<sup>4</sup>

*In this paper the thermal effects on the positioning accuracy of ABB IRB 140 industrial robot are studied with the help of finite element analysis (FEA) and Ansys Workbench software application. Thermal behavior of the robot has been monitored for a work cycle of about 3 hours at a speed of 60% of robot maximum. Data recorded with the help of temperature sensors and infrared camera have been introduced as input parameters in FEA Simulation. The results have shown that thermal effects have a huge impact on robot's positioning accuracy, obtaining a total deformation of 0.097 mm at the robot's end flange.*

**Keywords:** industrial robot ABB IRB 140, precision, thermal deformation, FEA.

### **1. Introduction**

In recent years, industrial robots are increasingly present in applications that require high accuracy such as machining operations or measurement and control operations. Quality of the robotic processes or products resulted from robotic applications are highly influenced by the robot's performances. These performances are evaluated according to a series of parameters declared in the ISO 9283 standard, and there is a constant need and seek of improving them.

The performance of industrial robots is influenced by several factors (error factors), very well detailed in [1]. These include: geometric errors of robot components or installation errors, errors arising from the backlash in gear trains and elastic displacements due to external loads or loads generated at the robot operation time, errors due to components wear, errors generated by transducer resolution, errors caused by the mathematical model (geometric, cinematic), errors from programming (offline CAD/CAM and post-processing) and last but not least *temperature-induced errors*.

<sup>1</sup> Assistant Prof., PhD. Student, Eng., Dept. of Robotics and Production Systems, University POLITEHNICA of Bucharest, Romania, e-mail: cozmin.cristoiu@upb.ro

<sup>2</sup> Professor, PhD., Eng., Dept. of Robotics and Production Systems, University POLITEHNICA of Bucharest, Romania, e-mail: miron.zapciu@upb.ro

<sup>3</sup> Professor, PhD., Eng., Dept. of Robotics and Production Systems, University POLITEHNICA of Bucharest, Romania, e-mail: afnicolescu@yahoo.com

<sup>4</sup> Professor, PhD., Eng., Dept. of Robotics and Production Systems, University POLITEHNICA of Bucharest, Romania, e-mail: cristinapupaza@yahoo.co.uk

The temperature-induced errors are also the subject of this paper, which is based on doctoral studies performed by the first author of this paper. The final goal of studies is to elaborate a mathematical model able to compensate these errors, and FEA studies of the thermal behavior of the robot presented in this paper represents one important step in this direction. In order to compensate these errors, first they must be identified and calculated. There have been many trials by different approaches on this subject. For example, in [1] thermal behavior investigation of a Kuka KR20 was made with the help of an infrared camera and displacement sensors mounted on the robot flange and errors measured have been quantified as parameters using small displacement theory [2]. In other paper [3] thermal behavior is studied with the help of FEA and based on the virtual model of the robot. In [4] an infrared camera is also used for thermal recording. This time positioning errors are measured with the help of a laser-tracker that is mounted on the. The laser-tracker is set to point on a video camera with high resolution capable of sensing small deviations of the laser spot (deviations supposed to be caused by thermal deformations). These errors are further used into a predictive model that consider the temperature of the robot during operation.

These were just some examples of studies in which even though the methods of analysis are different all have a common point. Regardless of the chosen approach, it finally tries to improve the accuracy of the robot by software modifying the kinematic parameters of the robot. To do this, calibration / compensation procedures involve the elaboration of a mathematical model whose parameters correspond faithfully to the actual behavior of the robot. To achieve good precision values, you must consider the factors of influence (both internal and external) in the geometry modeling of the robot. This involves quantifying (by measuring) the effects of error sources on the robot's geometry [5]. These thermal errors are also studied in this paper for the robot model ABB IRB 140.

## 2. Aspects regarding the FEM analysis

Thermal analysis follows the calculation of the temperature distribution and of the other quantities that characterize the thermal state in an object: the amount of heat transferred or absorbed, the thermal gradient, the thermal flux. Often the thermal analysis is followed by a stress analysis, to determine the tensions due to the contractions or thermal expansion. In finite element structural analysis programs, heat transfer can be simulated by conduction, convection (for 3D, 2D or axial-symmetrical structures that come into contact with a liquid layer) or by radiation. The finite elements used in the thermal analysis have as degrees of freedom the nodal temperatures. Thermodynamic phenomena is characterized by the following characteristic units:

**Q** - The heat flow [W / m<sup>2</sup>] or the heat flow represents the amount of heat passing through a surface in the unit of time:

$$Q = \int_A q \, dA \quad (1)$$

A graphic representation of heat flow is depicted in figure 1.

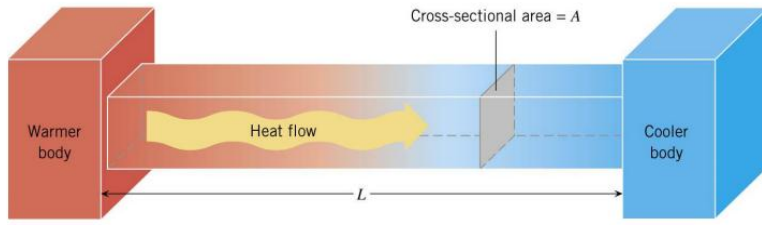


Fig. 1. Graphical representation of Q – The heat flow

where **q** - the unit heat flux (on the surface unit), in time, in the direction **n**, normal to the surface. The equation of the thermal conduction is:

$$q_n = -\lambda_n \frac{\partial T}{\partial n} \quad (2)$$

where  $\lambda_n$  - the thermal conductivity of the material in the direction **n** [W / m<sup>2</sup> °K].

It is determined experimentally and varies with the temperature.  $\frac{\partial T}{\partial n}$  is the temperature gradient in direction **n**. The energy generated in a 3D structure by a heat source is:

$$E_g = q_v V \quad (3)$$

where **qV** - the volume flow of heat, and **V** - the volume of the structure [m<sup>3</sup>].

The variation of the internal energy of the structure is:

$$\Delta E_{int} = \rho c V \frac{\partial T}{\partial t} \quad (4)$$

where  $\rho$  - density of material [kg / m<sup>3</sup>],  $c$  - specific heat of material [Ws / kg°K], **V** - volume of structure [m<sup>3</sup>], **T** - temperature [K] and **t** - time [s]. The law of energy conservation or thermodynamic equilibrium is described by the equation:

$$\Delta E_{int} + \sum E_c = \Delta E_i + \Delta E_g \quad (5)$$

where  $\Delta E_{int}$  - the variation of the internal energy,  $\sum E_c$  - the thermal energy transferred to the environment,  $\Delta E_i$  is the thermal energy from external sources,  $\Delta E_g$  - the energy generated from within the structure by a heat source. In the case

of heat transfer by conduction, the equilibrium equation (5), written on the basis of the principle of energy conservation becomes:

$$[C]\{\dot{T}\} + [K]\{T\} = \{Q\} \quad (6)$$

This means that: the sum of the internal energy and the energy transferred by conduction must be equal to the energy from external sources. In equation (6)  $[C]$  is the specific heat matrix,  $\{\dot{T}\}$  - derived with respect to the time of nodal temperatures,  $[K]$  - the thermal conductivity matrix,  $\{T\}$  - the vector of nodal temperatures, and  $\{Q\}$  - the vector of the heat flux coefficients of effective nodal. In this equation the primary unknowns are the nodal temperatures. The other sizes are calculated based on the nodal temperatures. Thermal analysis can be performed either stationary or transient. The analysis in stationary thermal regime is known as "steady-state thermal". This is used to determine the temperature distribution in a structure at thermal equilibrium. This analysis can be linear or nonlinear.

*a) Linear Analysis*

In linear analysis, time-dependent material properties are not considered, that is:  $\{\dot{T}\} = 0$  and  $[K] = \text{constant}$ . The structural equation is:

$$[K]\{T\} = \{Q\} \quad (7)$$

The system of simultaneous linear equations is solved by a single iteration. The system is used for conduction or convection and linear convection or conduction is applied.

*b) Nonlinear Analysis*

Material characteristics vary with temperature. The equation governing thermal analysis in nonlinear regime is: ( $i$  is the iteration number)

$$[K]\{T\} = \{Q\} \quad (8)$$

The first iteration solves the system of equations at the initial temperature, and the following iterations use the temperatures from the previous iteration to determine the conductivity matrix. The iterative process continues until convergence is achieved. The number of iterations required for a precise solution depends on the type of nonlinearity considered in the problem. The solution algorithm is Newton-Raphson. Thermal analysis in stationary or transient regime can be an initial condition for static-structural analysis. In this case, the

displacements or tensions due to the thermal demands are obtained. This simulation is a thermally-structural coupled analysis, or "multiphysics", because it allows the combination of two physical phenomena: thermal (described by the laws of thermodynamics) and mechanically (where the laws of classical mechanics apply). In the graphical interface of the Workbench project, the analysis connection is made interactive, by translating the different modules for which the connection is desired, or by Solution → Transfer data to New → Static Structural (figure 1).

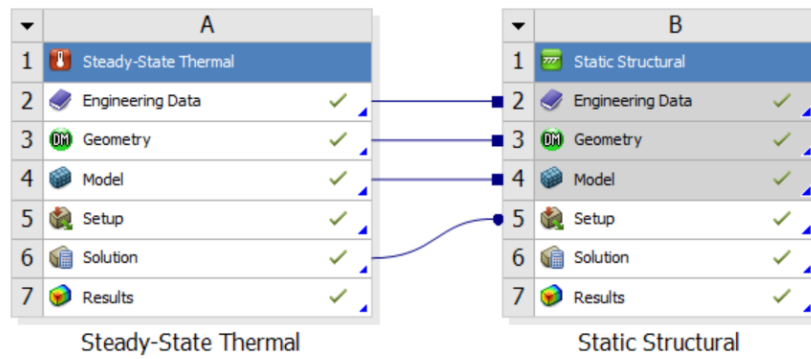


Fig. 1. Linking between thermal analysis and static structural

In order to make the static solution possible, the mechanical constraints corresponding to the static problem are introduced.

### 3. Geometric modeling, components and materials

For the thermal analysis by FEM to be a realistic one, 3 elements are essential to be correctly modeled and defined. The geometry of the analyzed geometric model must be as close as possible to the geometry of the real model. These types of computer simulations generally require very high computing power (high performance computers) and can last from hours to days or even whole weeks depending on the complexity of the analysis and the performance of the computers on which the simulation is performed. In order to shorten the computation times, a modeling stage is carried out to simplify the geometry of the virtual model, which is commonly called "defeaturing". In this defeaturing phase, geometrical elements that are not structurally significant (chamfers, blends, edges and faces with aesthetic role, sometimes holes) are eliminated. The difference of geometry, between the virtual model of the robot (as it is downloaded from the CAD base of the ABB manufacturer) and the simplified virtual model for the preparation of the FEM thermal analysis can be seen in figure 2.

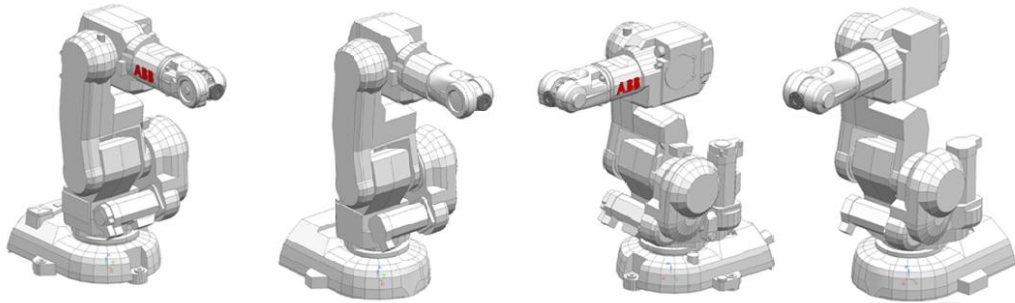


Fig. 2. Original and simplified CAD model of the robot prepared for FEA

A common feature of virtual models for industrial robots made available by most manufacturers is that they do not have the internal structure of the robot. Robot virtual models are modeled as solid blocks. These cannot be used as such for simulation because the static / dynamic behavior of such components is completely different from the structure elements of the "shell" type, as are the majority of the robot's components. In addition to editing the model and making structural elements in the form of thin-walled enclosures, the kinematic components and chains that they house must also be modeled. Between these components, the electric motors play the important role as heat sources and the components in the structure of the kinematic chains can drive the heat from the motors further into the structure, playing an important role in the thermal distribution. The difference between the original CAD model and the CAD model prepared for analysis can be seen in figure 3.

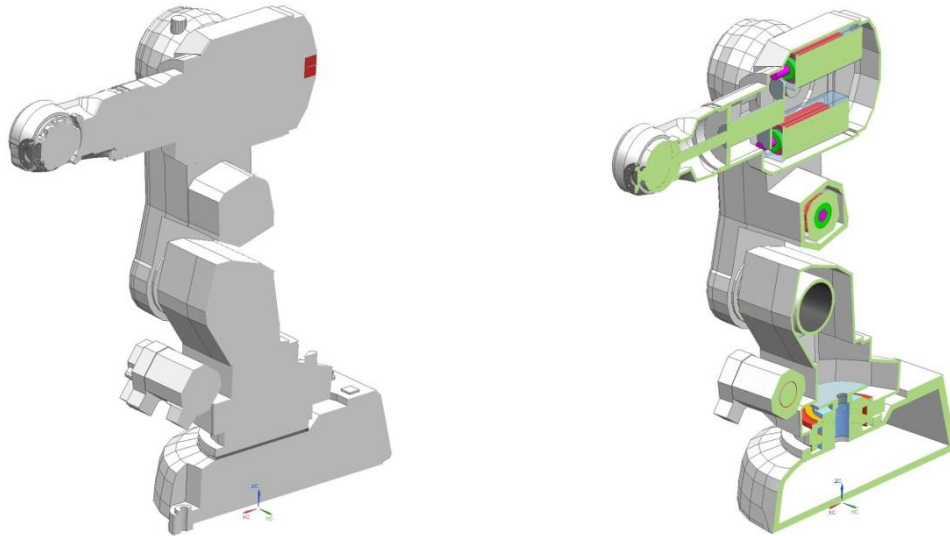


Fig. 3. Internal structure of robot modeled

Internal structure modeling was based on the information from the robot's product manual [6], information in the service manuals and spare parts and by direct measurements made on the real robot (with access by removing the covers from certain areas of the housing).

Motors modeling was done based on the information in their technical data sheets [7] [8], identifying the corresponding typo-dimensions for axes 1,2 and 3 with the L80-753026EBC motor and for the 4,5 and 6 axes with the L60-403026ENL-V2.0 motor. (brushless DC motors with integrated brake). The transmission of the movement for axes 1 and 2 is done by means of cycloidal reducers. Based on the measurements on the real model of the robot, the following types of reducers have been identified from the catalog [9]: NABTESCO RV10C. For axis 3, the transmission of the movement is realized by means of transmissions through the toothed belts and for the axes 4,5 and 6 by means of toothed gears and shafts that have been modeled as simplified elements such as discs / cylinders that come into contact simulating the gear and thus the transmission of heat through conduction. The positioning and numbering of the motors corresponding to each axis of the robot structure can be seen below in figure 4.

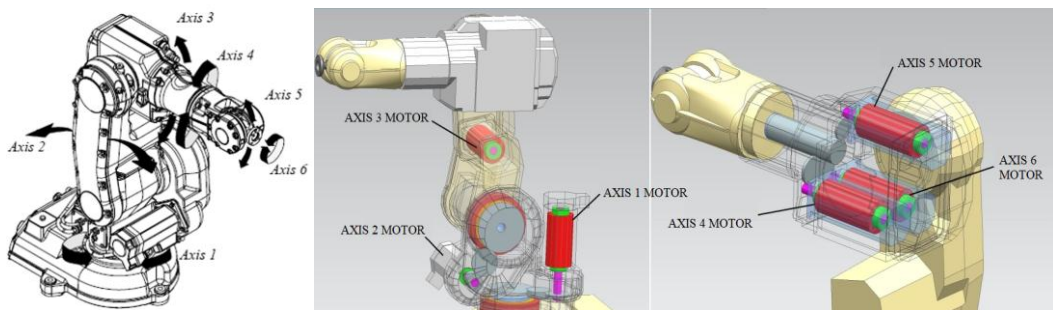


Fig. 4. Motors placement

Both the motors and the reducers were modeled as assemblies with complete internal structure (the internal elements such as rotor, stator, winding, bearings being simplified but still independently modeled) but keeping the dimensions and the assembly structure. Thus, for the different was possible to allocate different materials (exactly as in reality). The CAD model with all the internal structure is presented in figure 5.

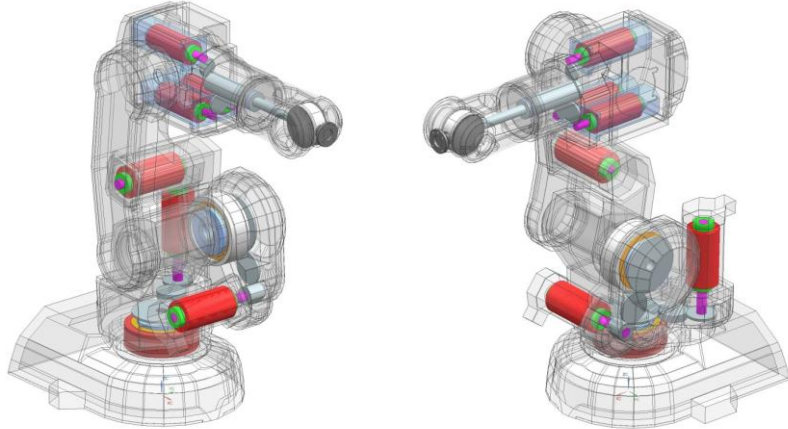


Fig. 5. Robot virtual model with full structure

Another essential element is the correct allocation of materials and material properties for the components of the assembly to be simulated. Apart from the material properties for copper (allocated to the motor windings) and the AlNiCo alloy (for magnets) taken from the ANSYS Workbench program database, all other material characteristics have been identified in the MatWeb database. MatWeb contains the mediated values of all material properties based on information received from thousands of manufacturers. For this reason, MatWeb is considered a database with reliable and realistic material features, which is used in design and research. The materials allocated to the components are:

- a) robot housing - Al A380
- b) gears, motor shaft, flange, pitch element, reducers - 18MoCrNi13
- c) bearings - A485 Steel, Grade 1
- d) magnets - AlNiCo
- e) windings – Cu

In the analysis, heat transfer through conduction and radiation was taken into account.

#### 4. Analysis results

The temperatures measured using the sensors placed directly on the motors [10] were used as input data for calibration of the FEM model. The maximum values recorded by temperature sensors for each motor (corresponding to each axis) of the robot are extracted in table 1.

**Table 1**  
**The maximum temperatures recorded with the help of thermocouples from the surface of the motors at 60% of robot maximum speed**

	Axis 1	Axis 2	Axis 3	Axis 4	Axis 5	Axis 6
Temp max [° C]	18.837	21.596	18.849	21.665	27.537	30.705

When importing the geometry into ANSYS Workbench, a coordinate system was automatically assigned, whose origin and orientation of the axes corresponds to the actual reference system, but the numbering of the axes is different. The coordinate system generated by ANSYS is the one presented in figure 6.

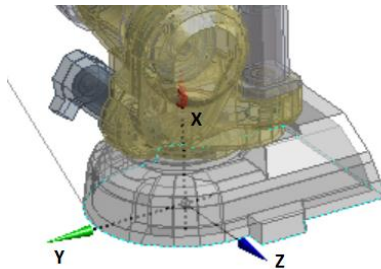


Fig. 6. ANSYS Axis System

Referred to this reference system attached to the base, the displacements of the mesh nodes chosen as diametrically opposed points on the contact surface of the rotating couples were recorded, for each structural element separately, determining their displacements. In the following figures 7, 8 and 9 the most important results are presented, the global map of the temperature distribution and the global map of the total deformations.

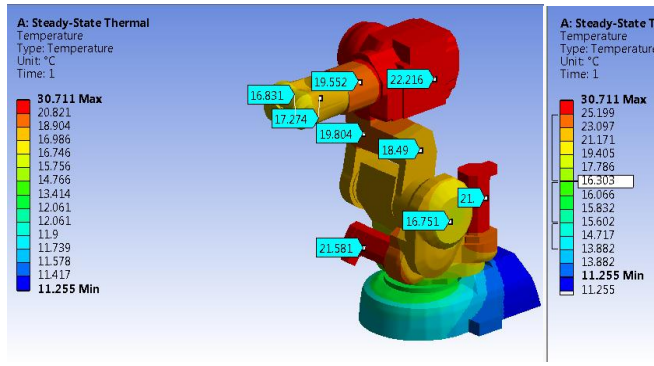


Fig. 7. ANSYS Heat transfer distribution

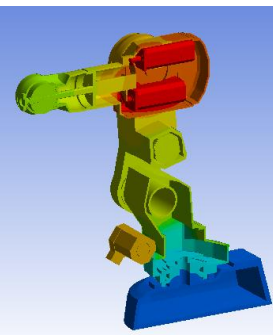


Fig. 8. ANSYS Internal heat distribution

The thermal analysis was performed under the conditions of the real operation of the robot (all axes operating). The observable effects regarding the way the robot structure is deformed are cumulative. The deformations of the individual elements in the robot structure are cumulative, the most important

effects being observable at the final element level (at the robot flange). Maximum total deformations of the structure cab be observed (as expected) at the end flange of the robot as depicted below in figure 9.

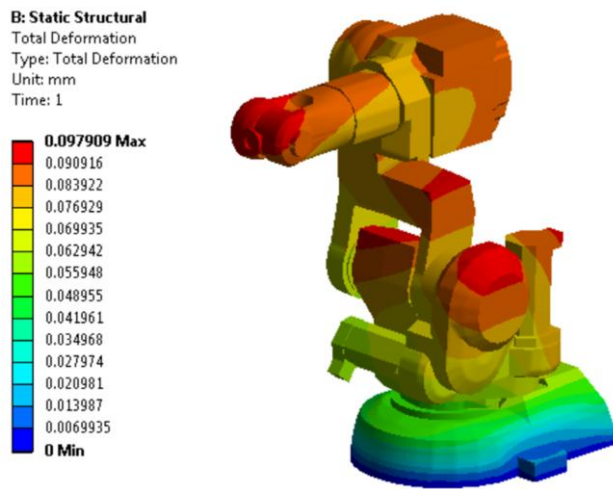


Fig. 9. Total deformations

Measured on the mesh at the flange surface, the directional displacements are:  
 $\Delta X = -0.0657$  mm,  $\Delta Y = 0.0474$  mm,  $\Delta Z = -0.0433$  mm.

Regarding the accuracy of FEA simulation results, conclusions are very difficult to formulate. On this subject, in [12], based on different case studies, it is pointed out that adopting the appropriate FEA modeling techniques achieves desirables results by maintaining a subtle balance between computational demands and result accuracy. In the absence of a reference model (i.e. an analytical calculated one), only the experience of the CAE specialist may assure that the results are correct. However, measurements made with the help of the laser-tracker in order to determine the repeatability of the robot indicate the fact that the results are appropriate. First measurements (after cold start of the robot) have shown a repeatability error of 0.04 mm. At the end of the measurements the error was of 0.143 mm. The position, configuration and robot parameters were not changed during the experimental sequences. The only factor that changed was the robot temperature gradients, indicating that the increase of the repeatability error from cold start to the end of measurements (difference of 0.104 mm) was mainly due to the thermal drift. Thus, if compared, FEA simulation results (0.097mm) fall into an error,  $\varepsilon = 6.7\%$ . However, it is necessary to underline the fact that FEA analysis was not intended for validating the model but instead it was carried out with the idea of offering a valuable insight of the thermal deformations weight with respect to the total positioning errors of the robot.

## 5. Conclusions

Thus, it is not the first analysis of robot behavior by FEA this is the first time when virtual model has been modeled to a such degree of similarity with the real model. Meanwhile most studies on this subject uses the virtual model as it is (a solid block) and with a single material applied in this case internal structure was modeled at the motor components level (even bearings, rotor, stator as separate parts with different and real materials applied in order to realistic simulate the thermal distribution in the robot structure). More than that the analysis model was calibrated, and results checked with data from previous work [10] where measurement real thermal behavior of the robot have been made (both with the infrared camera and with temperature sensors). The most important aspect is that for a type of robot, this kind of analysis can provide exactly the quantities needed in order to compensate thermal errors which are surprisingly significant even at lower temperatures. Real measurements of the robot have been made at an environment temperature of about 8°C and the maximum temperature measured on the robot was only about 30 °C. Thus, the directional deformations resulted by FEM are about  $\Delta X = -0.0657$  mm,  $\Delta Y = 0.0474$  mm,  $\Delta Z = -0.0433$  mm. Real position of the robot flange being shifted due thermal deformations as show in figure 10.

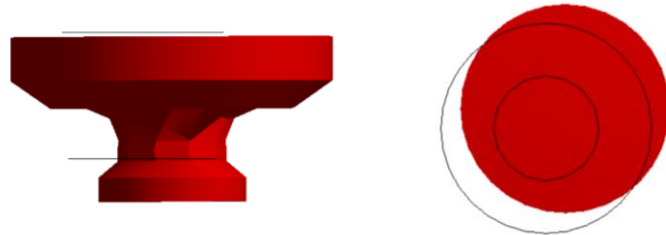


Fig. 10. Real displacement of the robot end-flange from its theoretic position

On the real robot, laser tracker measurements were also performed in [11] with respect to ISO 9283 and maximum positioning accuracy and repeatability errors were calculated of about: 0.558 mm and respectively 0.143 mm, meaning that thermal errors (0.097 mm), obtained from FEM analysis are responsible of about 17% of the positioning error and 68 % of the repeatability error. End flange directional displacements resulted from FEM analysis are the exact quantities that can be considered in a modified geometric model in order to compensate these thermal errors and improve the robot's accuracy by the factors mentioned. Every

robot has different structure, different heating curves and thermal stabilization times. Thus, it has been shown that this kind of thermal-structural FEM analysis can be used in order to identify thermal errors that can be used in a modified geometric/kinematic model in order to increase accuracy of an industrial robot. Such geometric model is under development for the robot ABB IRB 140 and a following paper will be published with results based on a compensation method based on these FEM analysis results on robot's thermal deformation and errors caused by it.

## R E F E R E N C E S

- [1]. *Mehdi C., Jean-Yves K., Alex B.*, "Thermal aspects on robot machining accuracy", Proceedings of IDMME – Virtual Concept 2010, France 2010
- [2]. *Bourdet P., Mathieu L., Lartigue C., Ballu A.*, "The concept of small displacement torsor in metrology", Series on Advances in Mathematics for Applied Sciences, Advanced mathematical tools in metrology II, vol. 40, pp.
- [3]. *C. Doukasa, J. Pandremenosa, P. Stavropoulosa, P. Foteinopoulosa, G. Chryssolourisa* " On an Empirical Investigation of the Structural Behavior of Robots " – ELSEVIER, Procedia CIRP 3 (2012 ) 501 – 506
- [4]. *Pranchalee Poonyapak, M. John D. Hayes* "Towards a Predictive Model for Temperature-Induced", Proceedings of EuCoMeS, the first European Conference on Mechanism Science Obergurgl (Austria), February 21–26 2006
- [5]. *Emanuele Lubrano*, "Calibration of Ultra-high-precision Robots Operating in an Unsteady Environment", These 5098, Faculte Sciences et Techniques de l'ingénieur laboratoire de systèmes robotiques, 2011
- [6]. \*\*\*ABB Product specification IRB140; Document ID: 3HAC041346-001; Copyright 2010-2017 ABB; [www.abb.com/robotics](http://www.abb.com/robotics)
- [7]. \*\*\*Technical data – ELMO DC BRUSHLESS MOTOR L60-403026ENL-V2.0  
<https://www.elmomc.com/product/servo-motors/>
- [8]. \*\*\*Technical data – ELMO DC BRUSHLESS MOTOR L80-753026EBC  
<https://www.elmomc.com/product/servo-motors/>
- [9]. \*\*\*Technical data – Nabtesco RV  
[http://www.motionusa.com.s3-website-us-east-1.amazonaws.com/nabtesco/RV-C\\_Series.pdf](http://www.motionusa.com.s3-website-us-east-1.amazonaws.com/nabtesco/RV-C_Series.pdf)
- [10]. *AF Nicolescu, C Cristoiu, C Dumitrascu, R Parpala*, "Recording procedure of thermal field distribution and temperature evolution on ABB IRB 140 industrial robot", IOP Conference Series: Materials Science and Engineering 444 (5), 052023
- [11]. *AF Nicolescu, C Cristoiu*, "Status check and calibration method for robot ABB IRB 140", IOP Conference Series: Materials Science and Engineering 444 (5), 052022
- [12]. *F.M. Ilie, T.G. Alexandru*, " The limiting aspects of product design software applied to the virtual prototyping of car body lifting end effectors", Annals of the University of Petroşani, Mechanical Engineering, 21 (2019), 59-64